

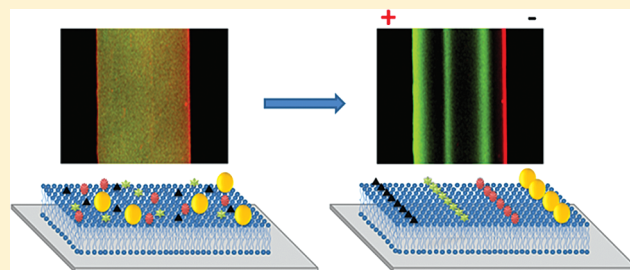
# Protein Separation by Electrophoretic–Electroosmotic Focusing on Supported Lipid Bilayers

Chunming Liu, Christopher F. Monson, Tinglu Yang, Hudson Pace, and Paul S. Cremer\*

Department of Chemistry, Texas A&M University, 3255 TAMU, College Station, Texas 77843, United States

**S** Supporting Information

**ABSTRACT:** An electrophoretic–electroosmotic focusing (EEF) method was developed and used to separate membrane-bound proteins and charged lipids based on their charge-to-size ratio from an initially homogeneous mixture. EEF uses opposing electrophoretic and electroosmotic forces to focus and separate proteins and lipids into narrow bands on supported lipid bilayers (SLBs). Membrane-associated species were focused into specific positions within the SLB in a highly repeatable fashion. The steady-state focusing positions of the proteins could be predicted and controlled by tuning experimental conditions, such as buffer pH, ionic strength, electric field, and temperature. Careful tuning of the variables should enable one to separate mixtures of membrane proteins with only subtle differences. The EEF technique was found to be an effective way to separate protein mixtures with low initial concentrations, and it overcame diffusive peak broadening to allow four bands to be separated simultaneously within a 380  $\mu\text{m}$  wide isolated supported membrane patch.



The extraction and separation of membrane proteins from cells has traditionally involved the use of detergents and sonication. Such methods, however, can destroy the native structures and activities of membrane proteins. This has led to a search for new methods for separating membrane proteins within supported lipid bilayer (SLB) environments, which should help preserve protein structure and activity.<sup>1–4</sup>

Separation experiments in supported bilayers have been performed by laminar flow, surface acoustic wave, and electrophoresis methods.<sup>5–8</sup> Electrophoretic techniques, pioneered by Sackmann's group,<sup>9</sup> have been used to manipulate fluorescently labeled lipids, membrane-bound proteins, and tethered lipid vesicles on SLBs.<sup>10–17</sup> For example, electrophoresis and electroosmosis have been employed to manipulate the migration of membrane-associated species in patterned SLB patches.<sup>12,13,16,17</sup> However, the separation of multiple components has been challenging. Several charged lipids were separated in SLBs with a method similar to gel electrophoresis.<sup>10</sup> The lipids separated based on their drift velocities in the electric field, which depended in part on the specific interactions between the analytes and the SLB matrix. Unfortunately, sample loading difficulties as well as peak broadening reduced the wide application of this method.

Herein, we report a novel method, electrophoretic–electroosmotic focusing (EEF), for bilayer species separation inspired by the isoelectric focusing technique.<sup>18</sup> EEF uses the electrophoretic force and an opposing electroosmotic gradient to focus negatively charged membrane-associated proteins and lipids from an entire SLB patch into narrow bands. The more negatively charged the molecule, the closer it will focus to the positive electrode, due to the larger electrophoretic contribution.

However, the larger the molecule's cross section within the aqueous solution, the closer the focusing position will be to the negative electrode, due to the electroosmotic contribution. The steady-state position of a given molecule results from the combination of these two physical characteristics, as illustrated in Figure 1. The EEF technique was found to be an effective way to separate protein mixtures with low initial concentrations, and it overcame diffusive peak broadening to allow many bands to be separated simultaneously within a single membrane.

## EXPERIMENTAL SECTION

**Materials.** Fibrinogen, streptavidin, and anti-biotin IgG were purchased from Sigma (St. Louis, MO). The latter two proteins were labeled according to procedures described previously.<sup>19</sup> 1-Palmitoyl-2-oleoyl-*sn*-glycero-3-phosphocholine (POPC), 1-palmitoyl-2-oleoyl-*sn*-glycero-3-phospho-(1'-rac-glycerol) (POPG), 1,2-dioleoyl-*sn*-glycero-3-phosphoethanolamine-*N*-(cap biotinyl) (biotin-cap-DOPE), and 1,2-dipalmitoyl-*sn*-glycero-3-phosphoethanolamine-*N*-(7-nitro-2-1,3-benzoxadiazol-4-yl) (NBD-DPPE) were purchased from Avanti Polar Lipids (Alabaster, AL). Poly(dimethylsiloxane) (PDMS) was obtained from Dow Corning (Sylgard, silicone elastomer-184).

**SLB Formation.** SLBs were formed by the vesicle fusion method<sup>20,21</sup> on clean glass coverslips (Corning, NY, 22 mm  $\times$  22 mm, no. 2). The coverslips were cleaned in a boiling 1:3

**Received:** July 8, 2011

**Accepted:** September 9, 2011

**Published:** September 29, 2011

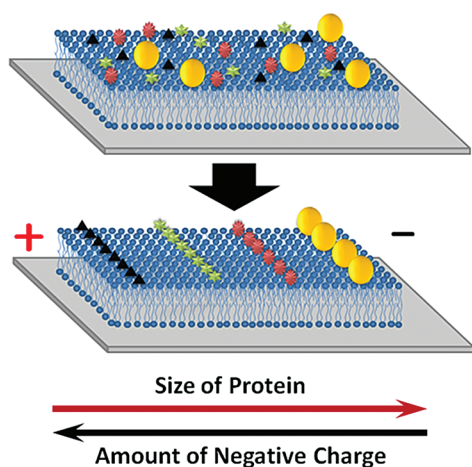


**Figure 1.** In EEF, an applied electric field focuses membrane-bound species from an initial disordered state (top) into bands (bottom). The focusing position depends on the size and charge of the species.

solution of 7X detergent (MP Biomedicals, Solon, OH) and purified water. Purified water came from an Ultrapure Water System (Thermo Scientific Barnstead Nanopure Life Science, Marietta, OH). The coverslips were rinsed with copious amounts of this water, dried with nitrogen, and annealed in a kiln at 500 °C for 5 h before use. Small unilamellar vesicles (SUVs) with 10% POPG, 0.5% NBD-DPPE, 1% biotin-cap-DOPE, and 88.5% POPC were prepared by vesicle extrusion. To do this, the lipids were mixed in chloroform. The chloroform was subsequently evaporated under a stream of nitrogen followed by vacuum desiccation for 4 h. Then the lipids were rehydrated in phosphate-buffered saline (PBS) solution which consisted of 10 mM sodium phosphate, 150 mM NaCl, and 0.2 mM sodium azide. The pH of the PBS solution was tuned to 7.4 with a small amount of 1 M HCl. The total concentration of the lipids in solution was 1.0 mg/mL. After several freeze–thaw cycles, the solutions were extruded through a polycarbonate filter (Whatman) with 100 nm pores.

**PDMS Stamp and SLB Patterning.** PDMS monomer and cross-linker were mixed in a 10:1 mass ratio. The mixture was stirred and vacuum-degassed. PDMS was then poured over a patterned glass mold and cured at room temperature overnight. The glass master consisted of a series of 10 380  $\mu\text{m}$  wide parallel lines that were 1 cm long and separated from one another by 200  $\mu\text{m}$  spacers. The glass master was prepared using standard HF etching techniques described previously.<sup>22</sup> The PDMS stamp was carefully peeled away from the glass, washed with ethanol, and rinsed with purified water. In all experiments performed herein, each SLB patch was about 380  $\mu\text{m}$  wide and isolated from the adjacent region by a fibrinogen monolayer adsorbed onto the planar glass substrate. To form SLB patches, a PDMS stamp was placed on a clean coverglass slide. A 1.0 mg/mL fibrinogen solution (in 10 mM PBS buffer) was added to form a fibrinogen monolayer on the exposed glass area. After a 1 h incubation, the fibrinogen was rinsed away with 10 mM Tris buffer, and the PDMS stamp was removed. Finally, 1 mg/mL lipid vesicle solution was introduced, and SLBs formed spontaneously on the area without the fibrinogen monolayer (Figure 2A).<sup>23</sup>

**Fluorescence Imaging and Flow Cell.** Epifluorescence images were obtained using a Nikon E800 fluorescence microscope with a Roper Scientific MicroMAX 1024B charge-coupled

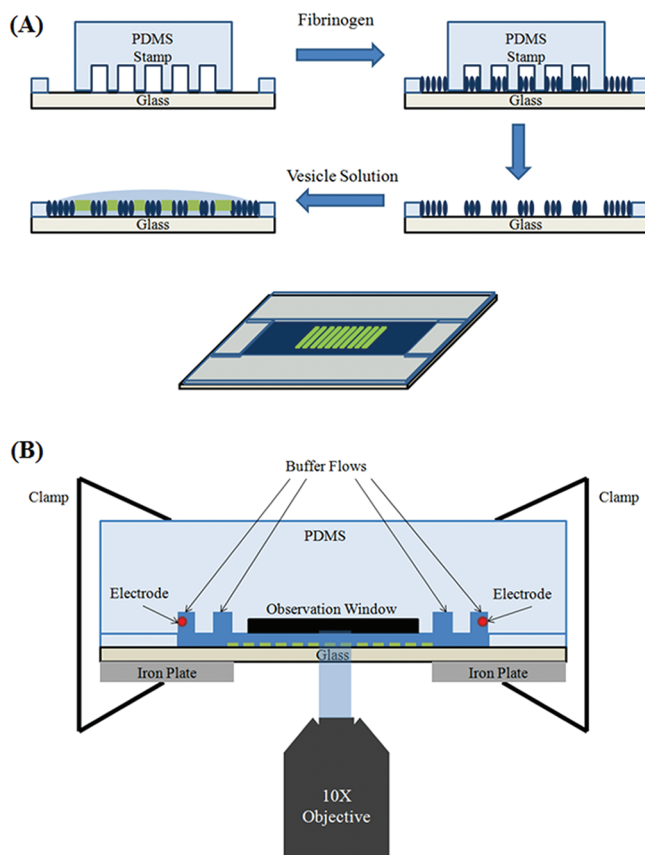


**Figure 2.** (A) Formation of patterned SLBs on glass. Each SLB patch was about 380  $\mu\text{m}$  wide and isolated from the adjacent region by a fibrinogen monolayer adsorbed to the planar glass substrate. (B) Side view of the flow cell. The distance between the two electrodes is 2 cm, and the length of the observation window is 1 cm. The distance between the top of the bottom glass slide and bottom of the observation window is about 100  $\mu\text{m}$ . The SLB is coated on the lower glass slide. The drawing is not to scale.

device (CCD) camera (Princeton Instruments). A flow cell described previously<sup>19</sup> was used to constantly control the pH and ionic strength over the course of an EEF experiment (Figure 2B). All experiments were performed with a 10 mM pH 7.3 Tris buffer. The buffer was flowed through the channels at a rate of 25 mL/h per channel.

## RESULTS

In a first experiment, streptavidin with four Alexa-488 dyes per molecule (StrA-4) was attached to the bilayer. This was done by incubating a 5 nM StrA-4 solution over the membrane for 30 min followed by the rinsing away of excess protein. The membrane-attached proteins were observed as a function of time at an applied field of 50 V/cm. (Figure 3A). As can be seen, the streptavidin, which is negatively charged at pH 7.3, was pushed toward the negative electrode (right) by the electroosmotic force in the first 5 min. However, it changed directions after 10 min and ultimately accumulated in a narrow band between the anodic edge and the middle of the patch. The origin of this behavior lies with the negatively charged POPG molecules, which move anodically (left) to form a gradient starting from the extreme left edge of the patch.<sup>11</sup> Initially, the POPG was uniformly distributed, and hence, the electroosmotic contribution was

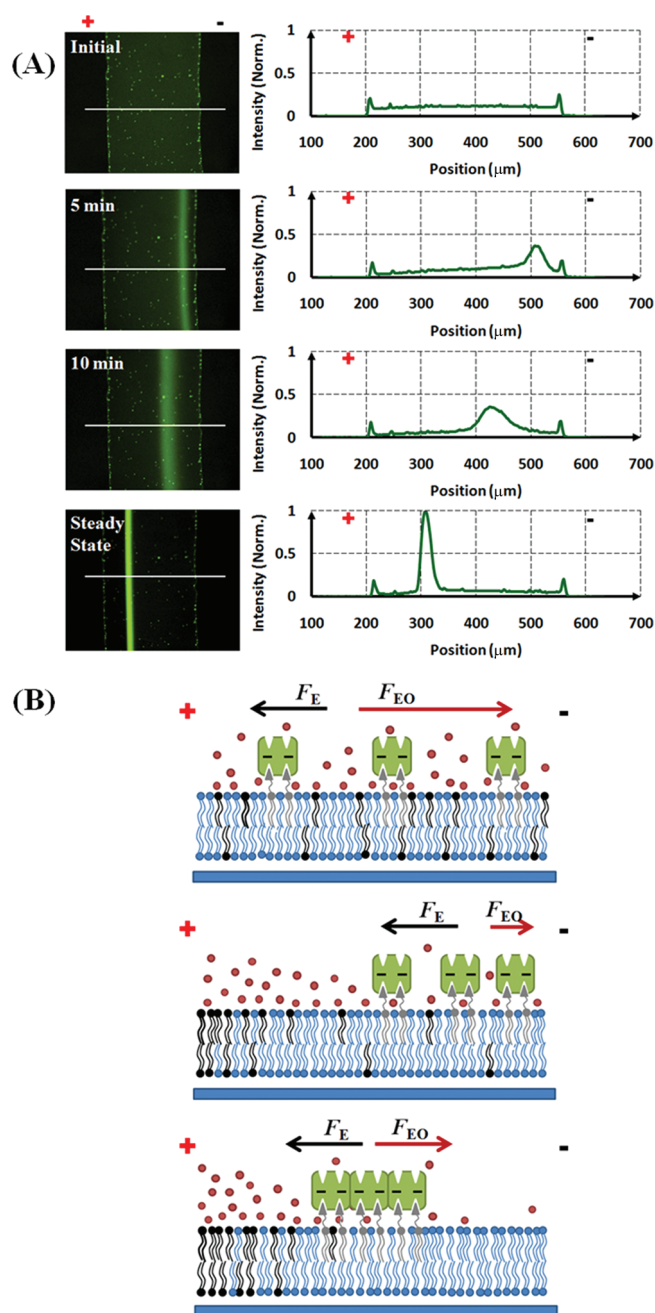


**Figure 3.** (A) Migration of StrA-4 in a lipid bilayer containing 10 mol % POPG with a 50 V/cm applied electric field. The pH was 7.3 and controlled by using 10 mM Tris buffer. The corresponding line scan profile is to the right of each image. The very small peaks along the edges were immobile proteins along the patch boundaries. (B) Schematic diagram of the migration of StrA in the bilayer.  $F_E$  is the electrophoretic force, and  $F_{EO}$  is electroosmotic contribution.

initially uniform over the entire patch, which caused the streptavidin to move to the right. Once the POPG gradient was established, however, the streptavidin moved electrophoretically to the left until the counterforce from the electroosmotic gradient exactly matched the electrophoretic contribution (Figure 3B). It should be noted that there are a few immobile bright spots in the micrograph. They are probably two-dimensional protein crystallites or aggregates that can

form on lipid bilayers under the appropriate pH and ionic strength conditions.<sup>24–26</sup>

Multiple proteins could be separated from one another and concentrated by exploiting the EEF method. This is demonstrated experimentally in Figure 4, where a negatively charged fluorescent lipid (NBD–DPPE), antibiotin IgG (labeled with two Alexa-594 per molecule), StrA-1 (streptavidin labeled with one Alexa-488 dyes per molecule), and StrA-4 were separated in the same SLB. After the biotin-containing SLB was prepared, the three proteins were premixed in solution (5 nM for StrA-1 and StrA-4 and 50 nM for the IgG) and incubated above it for 30 min. Excess protein molecules were washed away before fluorescence imaging. As can be seen, the protein concentration was initially uniform across the entire bilayer. However, after applying a 50 V/cm electric field for 1 h, the individual components migrated to their specific focusing positions.

As noted above, at steady state in an EEF experiment, there is a high POPG concentration near the anodic (left) edge of the SLB. This results in a high charge density at the anodic edge of the bilayer, and the charge density falls off to the right. Protein focusing takes advantage of this charge density gradient. The more negatively charged the protein, the closer it will focus to the positive electrode, due to the larger electrophoretic contribution. However, the larger the protein's cross section within the aqueous solution, the closer the focusing position will be to the negative electrode, due to the electroosmotic contribution. The steady-state position of any protein results from the combination of these two counteracting forces. During the protein labeling process, Alexa-488 reacts with primary amine groups on the proteins, principally at lysine residues. As such, StrA-4 carries a larger negative charge than StrA-1 because the Alexa-488 dye molecules bear a net charge of  $-2$  and replace the charge on the lysine, which was originally  $+1$ . Thus, for each labeled site, a net charge of  $-3$  is added while the electroosmotic profile is nearly unchanged.<sup>19</sup> Thus, StrA-1 and the StrA-4 are separated from one another on the basis of differing charges. IgG has a molecular weight of about 150 kDa, which is roughly 3 times greater than that of streptavidin. Therefore, the electroosmotic force on this protein is significantly larger and its motion is less dependent on its net charge. The estimated charge and radius of the proteins used in Figure 4 are listed in the first two columns of Table 1.

## DISCUSSION

The steady-state position of a protein can be modeled mathematically by taking into account its electroosmotic profile and its charge. Specifically, a protein comes to rest at the position where  $F_E + F_{EO} = 0$ . On the basis of the expressions for the electrophoretic and electroosmotic forces<sup>31</sup> one can write

$$\zeta_m = \zeta_{EO} \quad (1)$$

where  $\zeta_{EO}$  is the  $\zeta$ -potential of the SLB (planar surface with thin diffusive double layer), whereas  $\zeta_m$  describes the  $\zeta$ -potential of a membrane-bound protein. Using this expression, one can calculate the relationship between the charge density on the membrane surface at the focusing position and the physical properties of the protein. Specifically, the  $\zeta$ -potential is<sup>32</sup>

$$\zeta_m = \frac{Q_m \kappa^{-1}}{4\pi\epsilon r_m (\kappa^{-1} + r_m)} \quad (2)$$

where  $Q_m$  is the charge on the protein,  $r_m$  is the radius of the protein,  $\kappa^{-1}$  is the Debye length, and  $\epsilon$  is the permittivity of the



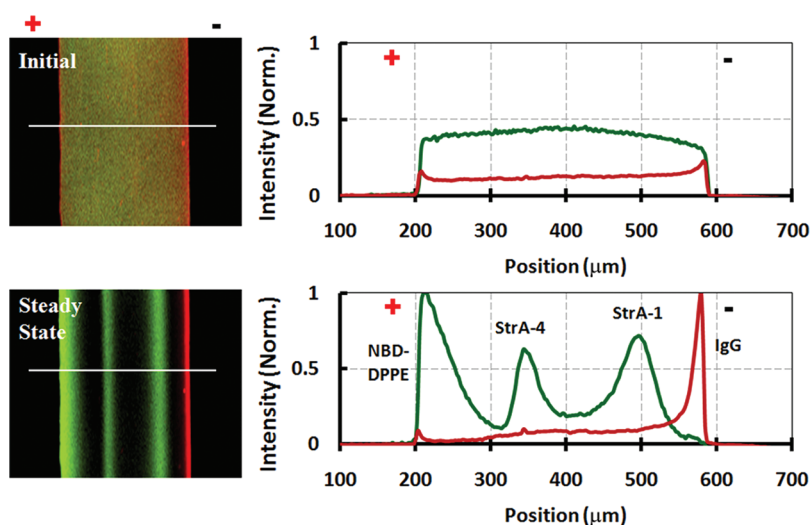


**Figure 4.** Separation of a protein and fluorescent lipid mixture in an SLB containing 10 mol % POPG. The solution was a 10 mM Tris buffer at pH 7.3. The top image shows the membrane before the field was applied. The bottom image was taken after the application of a 50 V/cm potential for 30 min. Adjacent to each image is the corresponding fluorescent line scan profile. The bands on the bottom image from left to right are NBD–DPPE, StrA-4, StrA-1, and anti-biotin IgG.

**Table 1.** Estimated Charge and Radius of Each Component in the EEF Separation Shown in Figure 4<sup>a</sup>

	charge ( $e^-$ ) $Q_m^b$	radius (nm) $r_m^c$	$\zeta$ -potential (mV) $\zeta_m$
StrA-4	16	2.5	−62.8
StrA-1	7	2.5	−27.5
IgG	4	4.5	−6.39

<sup>a</sup> The charge on a membrane-bound protein is the total charge on the labeled protein plus the charge on the bound biotin-cap–DOPE complex. Values for the charges and radii come from the associated references. <sup>b</sup> Refs 27 and 28. <sup>c</sup> Refs 29 and 30.

electrolyte medium ( $7.08 \times 10^{-10} \text{ F m}^{-1}$ ). At 298 K, the Debye length  $\kappa^{-1}$  is  $\sim 3 \text{ nm}$  in a 10 mM buffer. The calculated values of  $\zeta_m$  for each protein employed in Figure 4 are listed in Table 1.

The position-dependent  $\zeta$ -potential of the SLB surface is related to the surface charge density  $\sigma_x$  as<sup>32</sup>

$$\zeta_{EO} = \frac{\kappa^{-1} \sigma_x}{\epsilon} \quad (3)$$

Due to the POPG gradient, the charge density of the SLB,  $\sigma_l$ , is a function of the position,  $x$ , along the bilayer. An additional contribution,  $\sigma_g$ , comes from the charge on the glass substrate and is constant over the SLB. The total surface charge density  $\sigma_x$  is simply the summation of  $\sigma_l$  and  $\sigma_g$ . Thus,  $\sigma_x$  is a function of the lateral position along the SLB as<sup>12</sup>

$$\sigma_x = \sigma_g + \frac{\sigma_o}{\exp(-v_d(x - r_f)/D) + 1} \quad (4)$$

where  $\sigma_o$  is the initial charge density of the SLB in the absence of an applied field,  $v_d$  is the drift velocity of POPG in the electric field,  $x$  is the position in the SLB parallel to the electric field, and  $r_f$  is a constant with units of length and is related to the boundary conditions having the value of the width of the patterned bilayer section ( $380 \mu\text{m}$ ).  $D$  is the diffusion constant of POPG.

On the basis of eqs 3 and 4, the  $\zeta$ -potential of the SLB,  $\zeta_{EO}$ , at steady state can be plotted as a function of position along the

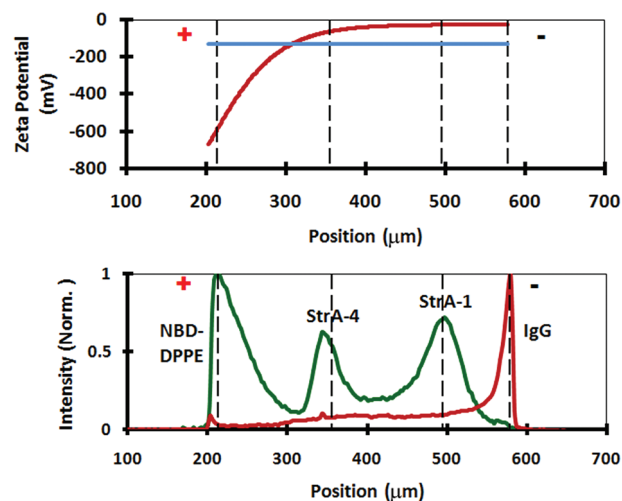


**Figure 5.** Top graph shows the  $\zeta$ -potential profile along a 10% POPG SLB before the application of an electric field (blue line) and at steady state after the application of a 50 V/cm field (red line). The dashed lines indicate the theoretical focusing positions of each component at steady state, as shown in Table 1. The bottom graph shows the fit of the calculated peak positions (vertical dashed lines) against the experimental line scan profile after separation from Figure 4.

direction of the electric field  $x$  (Figure 5, top, red curve).  $\sigma_o$  is calculated to be  $-24.3 \text{ mC/m}^2$  (see the Supporting Information), assuming the area of a lipid to be  $0.66 \text{ nm}^2$ .<sup>33</sup> Also,  $-6 \text{ mC/m}^2$  was used for  $\sigma_g$  and  $0.08 \mu\text{m}^2/\text{s}$  for  $v_d$  in a 50 V/cm electric field with  $D = 3.5 \mu\text{m}^2/\text{s}$ .<sup>9,17,34</sup> The focusing positions are determined by matching the  $\zeta$ -potential of the proteins calculated by eq 2 with the  $\zeta$ -potential of the SLB determined by eqs 3 and 4. Proteins focus where  $\zeta_m = \zeta_{EO}$ . The calculated focusing position of each component is marked by a vertical dashed line in Figure 5 and is in good agreement with the experimental data.

The initial migration direction of each charged membrane component can be predicted from the  $\zeta$ -potential before the

POPG is redistributed (Figure 5, top, blue line). Moreover, the eventual focusing  $\zeta$ -potential values of the proteins (red curve) are at smaller  $\zeta$ -potential values than the initial value at uniform 10% POPG distribution. As such, the initial migration of all proteins was dominated by their respective electroosmotic forces. The value of the surface  $\zeta$ -potential at the IgG focusing position was smaller than the value of the  $\zeta$ -potential contributed by the glass substrate ( $-25.8$  mV). Thus, this protein band was pushed to the right edge of the lipid bilayer. On the other hand, StrA-4 and StrA-1 first migrated one direction and then the other. NBD-DPPE did not protrude sufficiently far above the bilayer, so the electrophoretic force dominated the motion of the dye-labeled lipid under all conditions.

Combining eqs 2 and 3 reveals the relationship between the properties of each protein and its focusing position:

$$\frac{Q_m}{4\pi r_m(\kappa^{-1} + r_m)} = \sigma_x \quad (5)$$

As eq 5 indicates, the focusing position of a protein depends on the Debye length, which is related to the ionic strength of the buffer. Physically, this translates into a major change in the electroosmotic force. A protein's focusing position also depends on the charge on the protein, which can be varied by changing the solution pH. Equation 4 also indicates that the POPG gradient is affected by the drift velocity of this lipid as determined by the electric field strength. By modulating these factors, the focusing positions of protein bands can be shifted quite substantially (see the Supporting Information). Careful tuning of the separation conditions may allow the separation of complex mixtures of membrane proteins with only subtle differences.

In the future, the separation and focusing of transmembrane proteins perhaps from native cell membranes could be accomplished with polymer- or protein-cushioned SLBs.<sup>35–37</sup> EEF is ideally suited for work with trace membrane concentrations such as membrane proteins. This is because a large SLB area can provide for significant enrichment at the focusing location. Positively charged proteins could be separated in a similar manner as negatively charged species. In this case, the addition of positively charged lipids in an SLB would provide a positive charge gradient in an applied electric field. With sufficient positively charged lipid, the direction of electroosmotic flow could be switched, generating opposite electrophoretic and electroosmotic forces. In conclusion, we have demonstrated a new bilayer separation technique, EEF. This method can be used to separate, accumulate, and potentially identify many components in protein–lipid mixtures on charged supported lipid bilayers.

## ■ ASSOCIATED CONTENT

**Supporting Information.** Additional information concerning the focusing of proteins as a function of conditions, as well as extended calculations. This material is available free of charge via the Internet at <http://pubs.acs.org>.

## ■ AUTHOR INFORMATION

### Corresponding Author

\*E-mail: [Cremer@mail.chem.tamu.edu](mailto:Cremer@mail.chem.tamu.edu).

## ■ ACKNOWLEDGMENT

This work was funded by the National Institutes of Health (GM070622).

## ■ REFERENCES

- (1) Cristea, I. M.; Gaskell, S. J.; Whetton, A. D. *Blood* **2004**, 103, 3624.
- (2) Phizicky, E.; Bastiaens, P. I. H.; Zhu, H.; Snyder, M.; Fields, S. *Nature* **2003**, 422, 208.
- (3) Zheng, H. A.; Zhao, J.; Sheng, W. Y.; Xie, X. Q. *Biopolymers* **2006**, 83, 46.
- (4) Zhu, H.; Bilgin, M.; Bangham, R.; Hall, D.; Casamayor, A.; Bertone, P.; Lan, N.; Jansen, R.; Bidlingmaier, S.; Houfek, T.; Mitchell, T.; Miller, P.; Dean, R. A.; Gerstein, M.; Snyder, M. *Science* **2001**, 293, 2101.
- (5) Jönsson, P.; Beech, J. P.; Tegenfeldt, J. O.; Höök, F. *J. Am. Chem. Soc.* **2009**, 131, S294.
- (6) Nabika, H.; Sasaki, A.; Takimoto, B.; Sawai, Y.; He, S.; Murakoshi, K. *J. Am. Chem. Soc.* **2005**, 127, 16786.
- (7) Neumann, J.; Hennig, M.; Wixforth, A.; Manus, S.; Rädler, J. O.; Schneider, M. F. *Nano Lett.* **2010**, 10, 2903.
- (8) Nissen, J.; Gritsch, S.; Wiegand, G.; Rädler, J. O. *Eur. Phys. J. B* **1999**, 10, 335.
- (9) Stelzle, M.; Miehl, R.; Sackmann, E. *Biophys. J.* **1992**, 63, 1346.
- (10) Daniel, S.; Diaz, A. J.; Martinez, K. M.; Bench, B. J.; Albertorio, F.; Cremer, P. S. *J. Am. Chem. Soc.* **2007**, 129, 8072.
- (11) Groves, J. T.; Boxer, S. G. *Biophys. J.* **1995**, 69, 1972.
- (12) Groves, J. T.; Boxer, S. G.; McConnel, H. M. *Proc. Natl. Acad. Sci. U.S.A.* **1997**, 94, 13390.
- (13) Groves, J. T.; Wulff, C.; Boxer, S. G. *Biophys. J.* **1996**, 71, 2716.
- (14) Kam, L.; Boxer, S. G. *Langmuir* **2003**, 19, 1624.
- (15) van Oudenaarden, A.; Boxer, S. G. *Science* **1999**, 285, 1046.
- (16) Yoshina-Ishii, C.; Boxer, S. G. *Langmuir* **2006**, 22, 2384.
- (17) Han, X. J.; Cheetham, M. R.; Sheikh, K.; Olmsted, P. D.; Bushby, R. J.; Evans, S. D. *Integr. Biol.* **2009**, 1, 205.
- (18) Nelson, D. L.; Cox, M. M. *Lehninger Principles of Biochemistry*, 3rd ed.; Worth Publishers: New York, 2000.
- (19) Monson, C. F.; Pace, H.; Liu, C.; Cremer, P. S. *Anal. Chem.* **2011**, 83, 2090.
- (20) Brian, A. A.; McConnell, H. M. *Proc. Natl. Acad. Sci. U.S.A.* **1984**, 81, 6159.
- (21) Cremer, P. S.; Groves, J. T.; Kung, L. A.; Boxer, S. G. *Langmuir* **1999**, 15, 3893.
- (22) Shi, J. J.; Yang, T. L.; Kataoka, S.; Zhang, Y. J.; Diaz, A. J.; Cremer, P. S. *J. Am. Chem. Soc.* **2007**, 129, 5954.
- (23) Shi, J.; Yang, T.; Cremer, P. S. *Anal. Chem.* **2008**, 80, 6078.
- (24) Lou, C.; Shindel, M.; Graham, L.; Wang, S.-W. *Langmuir* **2008**, 24, 8111.
- (25) Lou, C.; Wang, Z.; Wang, S.-W. *Langmuir* **2007**, 23, 9752.
- (26) Ratanabankoon, P.; Gast, A. P. *Langmuir* **2002**, 19, 1794.
- (27) Prin, C.; Bene, M. C.; Gobert, B.; Montagne, P.; Faure, G. C. *Biochim. Biophys. Acta* **1995**, 1243, 287.
- (28) Sivasankar, S.; Subramaniam, S.; Leckband, D. *Proc. Natl. Acad. Sci. U.S.A.* **1998**, 95, 12961.
- (29) Schneider, S. W.; Lärmer, J.; Henderson, R. M.; Oberleithner, H. *Pflügers Arch.* **1998**, 435, 362.
- (30) Yan, H.; Park, S. H.; Finkelstein, G.; Reif, J. H.; LaBean, T. H. *Science* **2003**, 301, 1882.
- (31) McLaughlin, S.; Poo, M. M. *Biophys. J.* **1981**, 34, 85.
- (32) Shaw, D. J. *Introduction to Colloid and Surface Chemistry*, 3rd ed.; Butterworth & Co. Ltd.: U.K., 1980.
- (33) Poger, D.; Mark, A. E. *J. Chem. Theory Comput.* **2010**, 6, 325.
- (34) Behrens, S. H.; Grier, D. G. *J. Chem. Phys.* **2001**, 115, 6716.
- (35) Castellana, E. T.; Cremer, P. S. *Surf. Sci. Rep.* **2006**, 61, 429.
- (36) Diaz, A. J.; Albertorio, F.; Daniel, S.; Cremer, P. S. *Langmuir* **2008**, 24, 6820.
- (37) Tanaka, M.; Sackmann, E. *Nature* **2005**, 437, 656.